Journal of Chromatography, 609 (1992) 19–33
Elsevier Science Publishers B.V., Amsterdam

CHROM. 24 366

Shock layer thickness in the case of wide bands of single components and binary mixtures in non-linear liquid chromatography

Zidu Ma and Georges Guiochon

Department of Chemistry, University of Tennessee, Knoxville, TN 37996-1501, and Division of Analytical Chemistry, Oak Ridge National Laboratory, Oak Ridge, TN 37831-6120 (USA)

(First received January 28th, 1992; revised manuscript received May 21st, 1992)

ABSTRACT

The ideal model predicts the formation of a concentration shock on one side of an elution band, depending on the curvature of the isotherm. However, when a real column is used, a true concentration shock cannot form and a very steep boundary occurs instead, which is called a shock layer. It propagates at the same velocity as the ideal shock. The thickness of the shock layer has been defined and calculated by Rhee and co-workers in the case when the injection profile is a rectangular band wide enough for the elution profile to contain a constant state, *i.e.*, a plateau at the injection composition. This result is used to investigate the properties of binary frontal analysis in chromatography. Experimental results are in good agreement with the theory.

INTRODUCTION

When large-size samples are injected into a chromatographic column and the equilibrium isotherms of the sample components are not linear, the elution band profile is highly unsymmetrical. The theory of ideal, non-linear chromatography (assuming an infinite column efficiency) predicts a very different behavior for the two sides of the band. One side is diffuse. A self-sharpening effect, leading eventually to the formation of a concentration discontinuity or shock, takes place on the other side of the elution band [1–8]. This result is explained by considering the profile of a band moving along an ideal column as a concentration wave [4–7,9].

The ideal model predicts that under isothermal, isocratic conditions, each concentration moves at a constant velocity [1–4,7–10]. The velocity associated with a concentration depends on the slope of the equilibrium isotherm for this concentration, and increases with decreasing slope of the isotherm. Hence, for a convex upward isotherm, the concentration velocity increases with increasing concentration. However, high concentrations cannot pass low ones. When this phenomenon tends to occur, the band acquires a front concentration discontinuity instead [4,7,8,11]. Conversely, if the isotherm is convex downward, a discontinuity appears on the band rear. In the wave theory, these discontinuities are called shocks or shock waves [1,4–8].

Actually, chromatography can never be carried under the ideal model conditions. Although the efficiency of modern columns is high, it is never infinite as postulated by the ideal model, but remains finite. The separation process is not described by the ideal model but by the non-ideal, equilibrium-dispersive model [1–4,8,12–15]. This model predicts an erosion or smoothing of the discontinuity, resulting in a steady-state layer in which the concentration varies very steeply. This thin layer is called a shock layer [1,5–8,12–15]. It is centered on the shock

Correspondence to: Dr. G. Guiochon, Department of Chemistry, University of Tennessee, Knoxville, TN 37996-1501, USA.

0021-9673/92/$05.00

predicted by the ideal model and travels at the same velocity [12–14].

The formation of shock layers results from the competitive influence of two phenomena, one of thermodynamic and the other of kinetic origin. The phenomenon has been studied in detail by Rhee and co-workers [12–15] from a theoretical viewpoint. On the one hand, as just explained, different concentrations propagate at different velocities because of the non-linear behavior of the isotherm. Because there can be only one concentration value at a given time in a given point of the column, concentrations tend to pile up either at the front (convex upward isotherm) or the rear (convex downward isotherm) of the band. The corresponding part of the profile becomes steeper and steeper and a discontinuity would form, but for the finite column efficiency. On the other hand, the concentration gradient at a discontinuity would be infinite, which creates (Fick's law) an infinite flux of axial diffusion; the rate of mass transfers in the column is finite and this does not permit the propagation of a concentration discontinuity, *i.e.*, of an instantaneous change in concentration.

Thus, at the band boundary resulting from the competition between the sharpening thermodynamic process and the dispersing kinetic process, a dynamic equilibrium or steady state is reached and a shock layer is formed. Because the phenomenon is related to the mass transfer kinetics, we can expect a relationship between the shock layer thickness and the column efficiency. The shape of the other band boundary is determined by the combination of the non-sharpening (or spreading) thermodynamic process and the dispersing kinetic process, both of which disperse the boundary. In the case of a single component, the above phenomena result simply in one boundary being self-sharpening and very steep, while the other is non-sharpening and tails. With two components, the general trend can still be observed, but with more complications [2–4,7–9,15, 16].

Shock layers play an important role in the practice of non-linear chromatography and especially in frontal analysis, in displacement chromatography and in overloaded elution. One of the many applications of a shock layer theory would be the prediction of the minimum column efficiency necessary for a correct measurement of competitive isotherms by frontal analysis. The observation of an intermediate plateau in the breakthrough curve of the binary mixture is necessary for the calculation of the amount of each solute adsorbed on the stationary phase, using an integral mass balance [17]. The formation of this intermediate plateau is not instantaneous with a column of finite efficiency [9,16–18]. If the time needed for the formation of the intermediate plateau is longer than the retention time of the lesser retained component, this plateau does not appear and the results of the isotherm measurement are erroneous. An interpolation method can be used [17,18], but some minimum efficiency is needed to ensure the necessary accuracy.

Other applications of a shock layer theory are in displacement and overloaded elution preparative chromatography. The yield of the separation run of a mixture in fractions of certain components having a given degree of purity is determined by the width of the intermediate zone between the two purified fractions, hence by the shock layer thickness for each component. Being able to predict the shock layer thickness would permit a rapid estimate of these yields.

In this paper, we discuss the mathematical concepts of shock and shock layer, show how these concepts can be used for practical applications and give a numerical study of the formation and stabilization of a shock layer. Finally, we discuss the dependence of the shock layer thickness and of the time needed for its formation on the height of the concentration jump and the column efficiency.

THEORY

A general model for the behavior of a multicomponent mixture in a chromatographic column is obtained by combining the mass balance equation for each component of the system and the kinetic equations relating the rate of variation of the concentration of each component in the stationary phase to the concentrations of all the components in both phases. The mass balance is written as

$$\frac{\partial c_i}{\partial t} + F \cdot \frac{\partial q_i}{\partial t} + u_0 \cdot \frac{\partial c_i}{\partial x} = D_{a,i} \cdot \frac{\partial^2 c_i}{\partial x^2} \qquad (1)$$

where c_i and q_i are the concentrations of component i in the mobile and the stationary phase, respectively, $F = (1 - \varepsilon)/\varepsilon$ is the phase ratio, u_0 is the linear

velocity of the mobile phase and $D_{a,i}$ is the apparent dispersion coefficient. We shall assume here that the column efficiency exceeds 100 theoretical plates, so that the solution of the problem is identical with the solution of the equilibrium-dispersive model [4,8]. In this latter model, the concentration in the stationary phase is given by the equilibrium isotherm [$q_i = q_i(c_1, c_2, \ldots, c_k)$ for a k-component mixture] and the influence of the finite column efficiency, due to the axial dispersion and the finite rate of the kinetics of mass transfers, is accounted for by using a proper apparent dispersion coefficient in the right-hand side of eqn. 1. We see later in the discussion the extent of the validity of the equilibrium-dispersive model and its limitations.

The integration of the system of partial differential equations such as eqns. 1 written for each component of the mixture requires initial and boundary conditions. Typical conditions are

$$c_i(t,x = 0) = \phi_i(t) \tag{2}$$

$$c_i(t = 0,x) = 0 \tag{3}$$

$$i = 1,2$$

where $\phi_i(\cdot)$ is the boundary condition of the problem or concentration profile of each component at the column inlet. In elution, it is a pulse called the injection profile and often represented by an impulse (Dirac problem). In frontal analysis, it is a concentration jump (Riemann problem). When a rectangular band of concentrations C_i^0 and width t_p is injected, and t_p is large enough that the elution profile contains a constant state, *i.e.*, a plateau at C_i^0, the solution is practically equivalent to that of two successive Riemann problems corresponding to concentration jumps of the same magnitude and opposite signs.

In the particular case of this study, q_i is related to the mobile phase concentration of the two solutes, c_1 and c_2, through the competitive Langmuir isotherm:

$$q_i = \frac{a_i c_i}{1 + \sum_{j=1}^{2} b_j c_j} \qquad a_i = q_{s,i} b_i \tag{4a}$$

or

$$Q_i = \frac{C_i}{1 + \sum_{j=1}^{2} C_i} \qquad i = 1,2 \tag{4b}$$

where $C_i = b_i c_i$ and $Q_i = q_i/q_{s,i}$. For the sake of clarity in the forthcoming equations, we denote by C_i and Q_i the dimensionless concentrations of the ith component in the mobile and the stationary phases, respectively. Eqns. 4 are thermodynamically consistent only if $q_{s1} = q_{s2}$ (case of certain enantiomeric separations [19]). Otherwise, the Levan–Vermeulen competitive isotherm [20] must be used and only numerical solutions are possible.

The concentration profile through the shock layer can be calculated analytically in the case of a breakthrough curve and a Langmuir (single component [12–14]) or a competitive Langmuir (binary mixture [15]) isotherm. The demonstration is briefly summarized in the next section for convenience.

Shock layer profile in the case of a single component

The study of the experimental conditions under which a breakthrough curve adopts a constant pattern behavior (*i.e.*, propagates unchanged) and of how long a time or distance of travel is required for it to approach this steady state goes back to the 1940s and the work of Thomas [21]. This work, and the results of other early studies, were summarized by Vermeulen [22]. Cooney and Lightfoot [23] established the constant pattern conditions and Thomas and Lombardi [24] gave experimental proofs of the validity of this work. Finally, Rhee and co-workers [12–15] derived an equation relating the shock layer thickness to the experimental parameters, provided that the kinetics of mass transfer are rapid and can be accounted for by a constant dispersion coefficient, D_a, which lumps axial dispersion and finite mass transfer kinetics. Although this is an approximation, it is consistent with the agreement previously reported between experimental band profiles and the prediction of the equilibrium-dispersive model in most cases of practical interest in preparative chromatography [19].

Let $\eta = x/U_s - t$, where U_s is the velocity of the shock [4]:

$$U_s = \frac{u_0}{1 + k'_0 \Delta Q/\Delta C} \tag{5}$$

where ΔQ and ΔC are the amplitudes of the concentration shock in the stationary and mobile phases, respectively, and $k'_0 = Fa$ is the column capacity factor (or retention factor). In practice, we shall consider either profiles along the column ($t =$

constant) or profiles at the column exit ($x = L$). We assume that the shock velocity is constant, *i.e.*, that we have reached a dynamic steady state. Then, the profile of the shock layer does not depend on time any longer, it depends only on η. For a single component, when the kinetics of mass transfer are infinitely fast, but apparent dispersion remains finite, eqn. 1 becomes

$$\frac{D_a}{u_0 U_s^2}\cdot\frac{d^2C}{d\eta^2} - \frac{1}{U_s}\cdot\frac{dC}{d\eta} + \frac{1}{u_0}\left(1 + k'_0\cdot\frac{dQ}{dC}\right)\frac{dC}{d\eta} = 0 \quad (6)$$

It is known that in the case of a convex-upward isotherm, a front shock layer appears on the breakthrough curve and stabilizes [4,7]. When η tends towards $-\infty$ or $+\infty$, C tends towards C_0 or 0, respectively, and in both cases the differential $dC/d\eta$ tends towards 0. Eqn. 6 can be integrated and we obtain [15]

$$\Delta\eta = D_a\cdot\frac{(1+K)^2}{u_0^2 K}\cdot \left(\frac{C_0+1}{C_0}\cdot\ln\left|\frac{C_r - C_0}{C_l - C_0}\right| - \frac{1}{C_0}\cdot\ln\left|\frac{C_r}{C_l}\right|\right) \quad (7)$$

where $\Delta\eta$ is the time between the moments when the component concentrations are C_l and C_r at the column outlet, respectively, C_0 is the dimensionless mobile phase concentration at the injection, D_a is the apparent axial dispersion coefficient accounting for the deviations from the ideal equilibrium theory and

$$K = k'_0/(1 + C_0) \quad (8a)$$

is the amount adsorbed by the stationary phase at equilibrium between the two phases. The isotherm is given by eqn. 4b, for a single component. As a first approximation, we could assume that

$$D_a = Hu_0/2 \quad (8b)$$

where H is the column height equivalent to a theoretical plate. It would probably be more exact to use another equation, derived previously in an investigation of the kinetic models of chromatography (ref. 25, eqn. 19), and which gives a different weight to the axial dispersion and the mass transfer resistance terms than the conventional HETP equation of linear chromatography. However, this question deserves a more thorough investigation, currently undergone in connection with an experimental study.

Obviously, eqn. 7 gives the concentration profile across the shock layer. This profile is symmetrical, which is due to the assumption of a constant dispersion coefficient. Experiments show the validity of this conclusion in most practical cases, as long as the column efficiency is not very low. In theory, eqn. 7 only applies to the wave in an infinitely long column. We can record the profile as it moves past

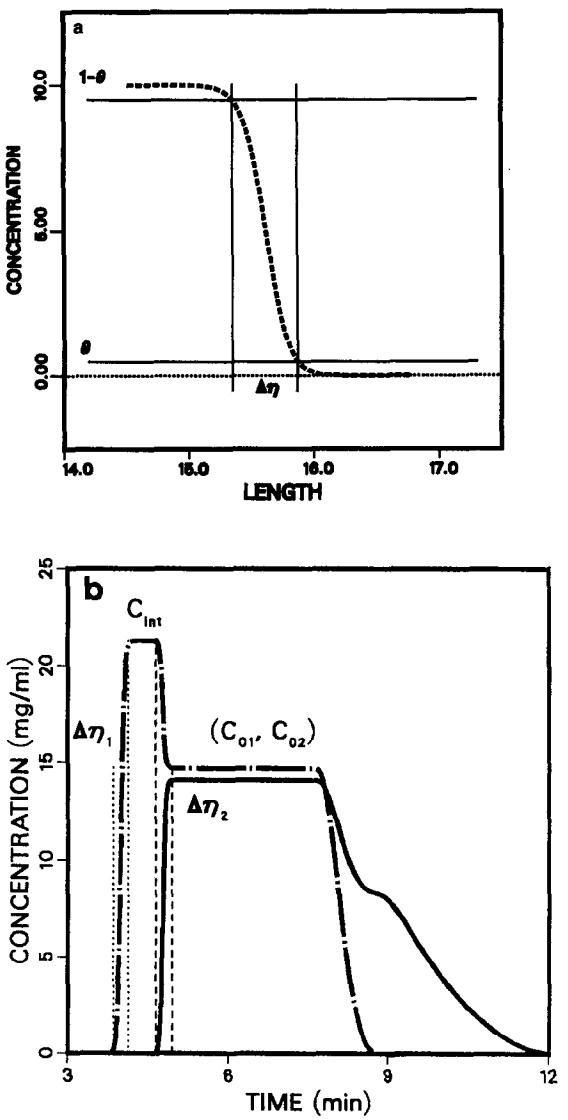

Fig. 1. Schematic diagrams of the shock layer profile and definition of the symbols introduced. (a) Single-component case; (b) two-component case. Length in cm.

certain positions along this column and follow the trend towards an asymptotic profile.

The thickness of the shock layer as given by eqn. 7 depends on the choice of the concentrations C_l and C_r. It is convenient to define and use the following parameter:

$$\theta = \frac{C_l^* - C_l}{C_l^* - C_r^*} = \frac{C_r - C_r^*}{C_l^* - C_r^*} \tag{9}$$

Fig. 1 shows a schematic diagram of the shock layer profile and of the symbols just defined. In the case of the injection of a concentration plateau, C_0, into an empty column, $C_l^* = C_0$ and $C_r^* = 0$, so $C_l = (1 - \theta)C_0$. As expected for an actual column, it takes an infinite time to achieve the total concentration variation, from C_l^* to C_r^*, *i.e.*, for $\theta = 0$, the thickness of the shock layer is infinite. On the other hand, for $C_l = C_r = C_m$, $\theta = 1/2$ and the thickness is 0. For small but finite values of θ, the thickness of the shock layer is finite and is given by

$$\Delta\eta(\theta) = \frac{H(1+K)^2}{2u_0K} \cdot \frac{2 + C_0}{C_0} \cdot \ln\left|\frac{1-\theta}{\theta}\right| \approx \frac{H(1+K)^2}{2u_0K} \cdot \frac{2 + C_0}{C_0} |\ln\theta| \tag{10}$$

Finally, we note that to derive the thickness of the shock layer along the column or in time units, we need to project the thickness $\Delta\eta$, calculated along the η axis, on the corresponding, length or time, coordinate axis.

Shock layer profile in the case of two components

In the case of two components, the apparent dispersion (molecular and eddy diffusion) and the resistance to mass transfer between the two phases both contribute to the thickness of the shock layer [15]. Rhee and Amundson [15] have shown that if the column efficiency is finite because either the kinetics of mass transfer are infinitely fast and the axial dispersion is finite, or the axial dispersion is negligible but the rate of the mass transfer kinetics is finite, the profile of the shock layer can be integrated in closed form. However, when both the axial dispersion and the mass transfer kinetic contributions to the column efficiency are significant, which is most often the case in chromatography, there is no closed-form solution. A numerical solution only can be derived.

In the case of a wide rectangular injection band or a step input, we have a simple wave solution for the breakthrough front [4,5,8,15,16]. When the mass transfer kinetics are infinitely fast and the equilibrium isotherm is convex upwards, concentration shocks take place in the front boundary of the profiles [4,15]. The following relationship results from the simple wave solution of the system of eqns. 1 for two components, $i = 1,2$:

$$c_1 = \xi c_2 + A \tag{11}$$

where ξ satisfies the following equation [4–6,8,16]:

$$\xi^2 f_{21} + \xi(f_{22} - f_{11}) - f_{12} = 0 \tag{12a}$$

where

$$\xi = \frac{dc_1}{dc_2}, f_{ij} = \frac{\partial q_i}{\partial c_j} \text{ with } i,j = 1,2 \tag{12b}$$

Eqn. 12a is a general relationship which holds for any kind of isotherm function (Appendix I); ξ is known whenever the isotherm function is available.

In the case of the Langmuir isotherm (eqns. 4), however, ξ and A in eqn. 11 are constant for a given experiment, *i.e.*, they depend only on the concentrations C_1^0, C_2^0 of the wide rectangular injection pulse. Then, eqn. 11 becomes

$$c_1 = \xi c_2 + \frac{a_1 - a_2}{a_2 b_1 + a_1 b_2/\xi} \tag{13}$$

Using eqn. 8, we can rewrite the isotherm of the second component (eqn. 4, $i = 2$) as follows:

$$q_2 = A_2 c_2/(1 + B_2 c_2) \tag{14}$$

with

$$A_2 = a_2/(1 + b_1 A) \tag{14a}$$

and

$$B_2 = (b_1\xi + b_2)/(1 + b_1 A) \tag{14b}$$

with

$$A = \frac{a_1 - a_2}{a_2 b_1 + a_1 b_2/\xi} = \frac{1 - \alpha}{\alpha b_1 + b_2/\xi} \tag{14c}$$

Thus, in the case of a simple wave solution (frontal analysis or wide rectangular injection), the competitive isotherm of the two solutes, when these isotherms are accounted for by the competitive Langmuir model, can be decoupled in the interactive

region [4–6,8,16]. Because separation takes place between the two components, as shown in Fig. 2, the profile of the shock layer at the front of the less retained component band is given by the same mass balance equation as in the single-component case with the single-component isotherm (eqn. 4), while the shock layer at the front of the more retained component band is given by the same form of the mass balance equation, but using the decoupled isotherm function (eqn. 14a):

$$\frac{D_a}{u_0 U_{s,2}^2}\cdot\frac{d^2C_2}{d\eta^2}-\frac{1}{U_{s,2}}\cdot\frac{dC_2}{d\eta}+\frac{1}{u_0}\left(1+K_0'\cdot\frac{dQ_2}{dC_2}\right)\frac{dC_2}{d\eta}=0 \qquad (15)$$

where

$$U_{s,2}=\frac{u_0}{1+K_0'\Delta Q_2/\Delta C_2} \qquad (16)$$

and $K_0' = FA_2$. Note that, in order to apply this concerted disturbance approach, we have to assume that the two dispersion coefficients, $D_{a,1}$ and $D_{a,2}$, are identical.

The shock layer thickness of the first component band is given by the same equation as used in the case of a single component (*i.e.*, eqn. 10), with a single-component isotherm function, provided, however, that the concentration of the intermediate plateau, $C_{1,m}$, be used instead of $C_{1,0}$. The shock layer thickness at the boundary between the two components is obtained also with eqn. 10, but using the isotherm parameters given above in eqns. 14 [15]. For concentration profiles along the column (t = constant), the less retained component profile drops from the intermediate concentration to zero with increasing abscissa, whereas for the more retained component it drops from $C_{2,0}$ to zero. Eqn. 6 can be used in the two-component case to calculate the thickness of the shock layers. The parameters of the single-component isotherm are used for the less retained component and the decoupled isotherm parameters for the more retained component.

The concentration profile of the rear shock layer of the first component band given in reduced units (*i.e.*, θ) is the same as the concentration profile of the front shock layer of the second component band, except that the change in concentration is negative for the first component and positive for the second.

Formation of the intermediate plateau in the frontal analysis of binary mixtures

When a step of a binary mixture is introduced into a column, the front of the first-component band moves faster than the front of a band of the same first component, pure, at the same concentration. This is the displacement effect. As a consequence, the concentration of the first component in the first part of the breakthrough front, where it is pure, exceeds the boundary concentration, $C_{1,0}$ (Fig. 2). Ideally, with an infinitely efficient column, the concentration plateau is reached immediately at injection. With a real column, the formation of this intermediate plateau is not instantaneous. It takes a certain time before a steady state is achieved for the front of the breakthrough curve. We can calculate this time if we know the dependence of the thickness of the shock layer on the experimental parameters, and especially on the column efficiency and the height of the concentration plateau injected into the column. Beyond that time, the shock layer profile remains identical and the plateau expands because the front shock layer propagates faster than the intermediate one. Hence, there is a minimum column efficiency below which the accurate determination of competitive isotherm by frontal analysis is not possible. The shock layer theory permits its determination.

At the front boundary of the breakthrough profile, the fluxes of both solutes caused by convection are

$$J_1 = c_{1,0}U_1 \qquad (17a)$$

$$J_2 = c_{2,0}U_2 \qquad (17b)$$

where the two shock velocities, U_1 and U_2 are

$$U_1=\frac{u_0}{1+F\Delta q_1/\Delta c_1} \qquad (18a)$$

$$U_2=\frac{u_0}{1+F\Delta q_2/\Delta c_2} \qquad (18b)$$

where Δc_i and Δq_i are the concentration jumps in the mobile phase and the stationary phase, respectively. The difference between the flux given by eqns. 17a and 17b gives the amount, n_1, of the less retained compound which is separated from the mixture and elutes pure, between the two shocks, after a certain

time Δt, has elapsed. It is

$$n_1 = \int_0^{\Delta t} (J_1 - J_2)\mathrm{d}t = (c_{1,0}U_1 - c_{2,0}U_2)\Delta t \qquad (19)$$

With a real column, the intermediate plateau does not appear instantaneously. As shown in Fig. 2, the amplitude of the first-component shock layer grows progressively, so a peak appears in front of the injection plateau. When the height of this peak becomes equal to the concentration of the intermediate plateau, the amount of the less retained compound which is between the two shock layers is

$$n_1 = \frac{1}{2}\Delta c_{\mathrm{int}}(\Delta\eta_1 + \Delta\eta_2) \qquad (20)$$

Combining eqns. 17 and 18 gives the following relationship:

$$\Delta t = \frac{1}{2} \cdot \frac{\Delta c_{\mathrm{int}}(\Delta\eta_1 + \Delta\eta_2)}{c_{1,0}U_1 - c_{2,0}U_2} \qquad (21)$$

where Δc_{int} is the difference between the first-component concentrations on the intermediate, enriched plateau and just before the injection; $c_{1,0}$ and $c_{2,0}$ are the concentrations of the two components after the injection. $\Delta\eta_1$ and $\Delta\eta_2$ are the thicknesses of the two shock layers in length units. Eqn. 21 is a useful approximation. A more exact relationship can be obtained (Appendix II).

Numerical calculations

For numerical calculations, a finite difference scheme was used [26,27]. The continuous plane z,t, in which the concentrations c_i are defined, is replaced by a grid $j\Delta z$, $\eta\Delta t$, where Δz and Δt are the space and time increments chosen for the integration and j and n are integers. The partial differential eqns. 1 are replaced by the finite difference equations

$$\frac{c_{i,j}^{n+1} - c_{i,j}^{n}}{\Delta t} + F \cdot \frac{q_{i,j}^{n+1} - q_{i,j}^{n}}{\Delta t} + u_0 \cdot \frac{c_{i,j}^{n} - c_{i,j-1}^{n}}{\Delta x} = 0 \qquad (22)$$

This equation defines a computation scheme which is implicit with respect to the unknown concentration [28]. By setting the time increment, Δt, to a small enough value, the numerical dispersion introduced in the calculations can be made relatively independent of the concentration because the simulated HETP is related to the time and space increment, in the case of single component, by the following equation [26]:

$$H = \Delta x - \frac{u_0\Delta t}{1 + F\mathrm{d}q/\mathrm{d}c} \qquad (23)$$

Then, the space increment can be set equal to H. The program is written in Fortran and run on the VAX8800 cluster of the UTCC.

The thickness of the shock layers of the profiles obtained by numerical calculations can be obtained either directly from the breakthrough curve, using eqn. 9 and interpolating linearly between the calculated points of the numerical solution, or by differentiating the front of the concentration profiles of the two solutes (Fig. 3), computing the second-order moment of these differential profiles which are nearly Gaussian and taking a value equal to four times the standard deviation corresponding to this variance.

For the numerical calculations discussed in this work, we have chosen a column length of 25 cm and a phase ratio $F = 0.35$. The hold-up time, t_0, is 3.00 min and the width of the rectangular injection plug is 4.50 min. In many instances the elution profile of the band tail, which is not relevant to this work, is not reported. Unless the influence of the column efficiency is studied, $H = 0.0125$ cm. Unless the influence of the height of the pulse is studied, $C_0 = 10$ mg/mL for both solutes. The isotherm parameters are $a_1 = 1.97$, $a_2 = 3.70$, $b_1 = 0.0396$ and $b_2 = 0.0411$. The relative retention of the two components under analytical conditions is 1.87. The ratio of the integration increments, $\delta t/\delta x$, was set equal to 0.2, unless the influence of that ratio was being studied (the Courant number is $u_z\delta t/\delta x$).

RESULTS AND DISCUSSION

We present successively the results of the numerical calculations explained in the previous section and a series of experimental results collected in frontal analysis, using equipment, products and procedures described previously [16,29] or separately [18]. The separation studied is that of 2-phenylethanol and 3-phenylpropanol on a 25 × 0.45 cm I.D. column packed with 10-μm particles of Vydac (Separations Group, Hesperia, CA, USA) C_{18} chemically bonded silica, with water–methanol

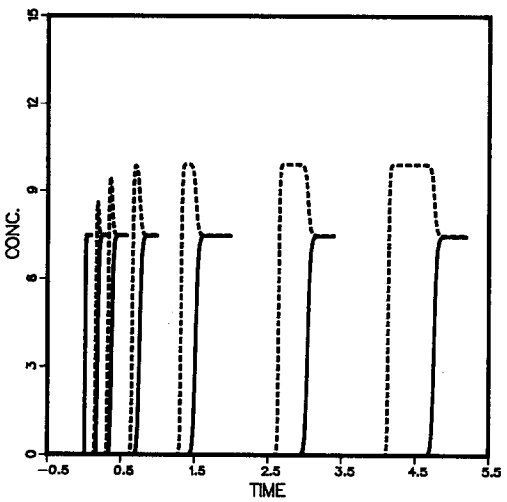

Fig. 2. Elution profiles at different column lengths. From left to right, 1 = 0.1 cm, 2 = 1 cm, 3 = 2 cm, 4 = 4 cm, 5 = 8 cm, 6 = 16 cm, 7 = 25 cm. The parameters used in the calculation are the same as in Table I. Solid line, more retained compound; dashed line, less retained compound. Column: L = 25 cm; H = 0.0125 cm; F = 0.35; hold-up time, t_0 = 3.00 min. Isotherm parameters: a_1 = 1.97; a_2 = 3.70; b_1 = 0.0792; b_2 = 0.0822. Sample concentration: C_0 = 7.5 mg/ml for both solutes. Time in min, concentrations in mg/ml.

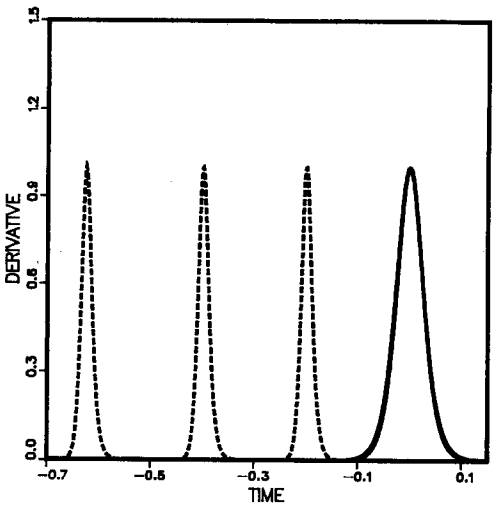

Fig. 3. Differentials of the fronts of last three sets of bands in Fig. 2. Solid line, more retained compound; dashed line, less retained compound. The origin of the time coordinate is at the front of the more retained compound, so differentials of the bands of the more retained compound are superimposed whereas those of the less retained compound are shifted. Units as in Fig. 2.

(50:50) as the mobile phase (1 ml/min). The column efficiency was 2500 theoretical plates for a very small injection of 3-phenylpropanol. Nearly rectangular plugs 4.5 min wide were injected.

Results of calculations

Fig. 2 shows the profiles of the breakthrough curves for the components of a binary mixture, at the exit of columns of increasing lengths. One can see the rapid stabilization of the two shock layers, a peak rising at the top of the first-component breakthrough curve and the gradual formation of the enriched plateau of the lesser retained component accompanying the separation of the fronts of the two solutes. Differentials of the shock layer profiles are shown in Fig. 3 for the last three breakthrough curves in Fig. 2. These three differentials nearly coincide in the case of the second component. Since

TABLE I

RETENTION TIME AND THICKNESS OF SHOCK LAYERS

$t_{R,1}$ and $t_{R,2}$ are the retention times of the lesser and the more retained components, respectively. The velocities of the ideal concentration shocks are $U_{s,1}$ = 5.7350 and $U_{s,2}$ = 4.8544 cm/s. L is the column length. The parameters used for the calculations are the same as those used for Fig. 4.

L (cm)	$t_{R,1}$ (min)	$t_{R,2}$ (min)	$\Delta\eta_1$ (min)	$\Delta\eta_2$ (min)	U_{s1} (cm/s)	U_{s2} (cm/s)
2	0.3439	0.4064	0.0515	0.0886	5.816	4.921
4	0.6917	0.8185	0.0601	0.1104	5.783	4.887
8	1.3890	1.6428	0.0628	0.1267	5.760	4.870
12	2.7839	3.2921	0.0632	0.1345	5.747	4.860
25	4.3547	5.1490	0.0651	0.1364	5.741	4.855

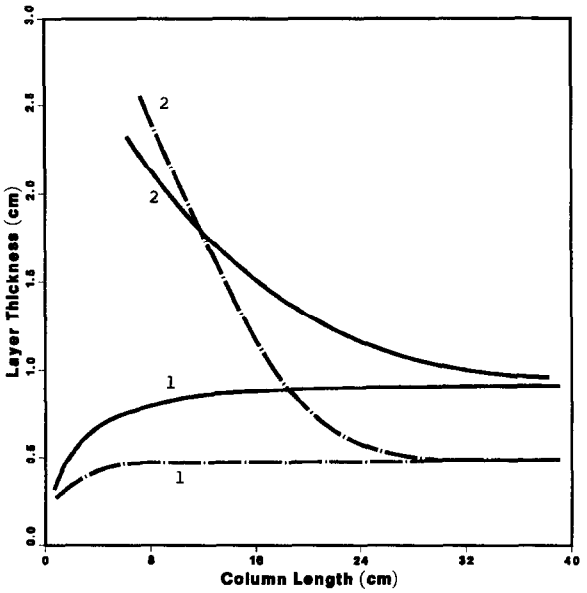

Fig. 4. Plot of the shock layer thickness *versus* the migration distance. Solid line, second front; dot-dashed line, first-component front. Lines 1, rectangular plug injection: lines 2, non-rectangular injection profile. Column: L = 25 cm; H = 0.0125 cm; F = 0.35; t_0 = 3.00 min. Isotherm parameters: a_1 = 1.97; a_2 = 3.70; b_1 = 0.0396; b_2 = 0.0411. Injection time: t_p = 4.50 min. Sample composition: C_0 = 10 mg/ml for both solutes.

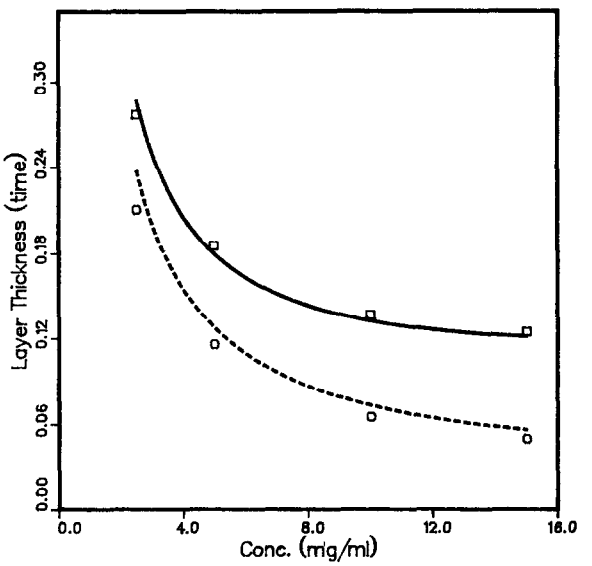

Fig. 5. Comparison of the shock layer thicknesses predicted by eqn. 10 (lines) and derived by numerical calculations (symbols) with different column loading concentrations. The thickness is in minutes. Solid line, more retained compound; dashed line, less retained compound. Calculation parameters as in Fig. 4.

the time origin is set at the center of the second shock layer, the distance between the two profiles increases with increasing column length and the differentials of the three profiles of the first-component breakthrough curves are almost identical but shifted. The values of the shock layer thicknesses are reported in Table I.

The injection profile is rectangular, *i.e.*, the front of the injection profile is a true shock and the initial thickness of the shock layer is zero. Because of the axial dispersion, the shocks of the two components separate, acquire round edges, a finite thickness which increases with increasing migration distance while the enriched plateau forms and reaches a stable height, defined by the isotherm function as shown in eqn. 8, and equal to A [16]. The shock layer profiles of both solutes tend rapidly towards a stable, steady-state shape, as shown in Fig. 3. The shock layer thickness tends towards a limit which is different for the two compounds (Fig. 4 and Table I). This behavior is profoundly different from what is observed in linear chromatography. In this last

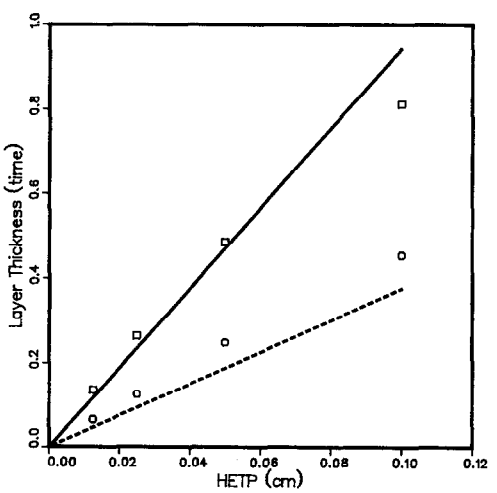

Fig. 6. Comparison of the shock layer thicknesses predicted by eqn. 10 (lines) and derived by numerical calculations (symbols) with columns having different efficiencies. The thickness is in minutes. Solid line, more retained compound; dashed line, less retained compound. Calculation parameters as in Fig. 4.

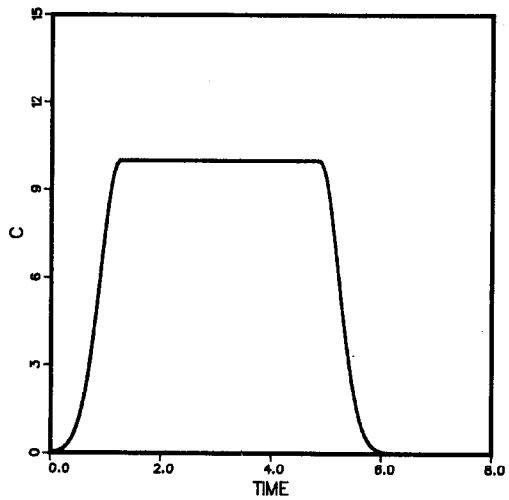

Fig. 7. Injection profile for the calculation of the diffused fronts. The other calculation parameters are the same as in Fig. 4. The injection concentration is 10 mg/ml for both solutes. Units as in Fig. 2.

case, the width of the front boundary of a profile is proportional to the square root of the column length and broadens constantly with increasing migration distance. In non-linear chromatography, in contrast, the thickness of the shock layer stabilizes rapidly when the enriched concentration plateau has been formed.

In Figs. 5 and 6 we compare the prediction of eqn. 10 for the thicknesses of the two shock layers and the results of the numerical calculations for the dependence of the thickness of the shock layer on either the height of the input concentration step (Fig. 5) or the column HETP (Fig. 6). The agreement is excellent. The minor discrepancies observed are due to numerical errors or result from the constraints of the numerical calculation of solutions of the chromatographic equations in the case of a binary mixture. These constraints have been discussed previously [26,27]. This problem is beyond the scope of the present study.

The calculations reported above were carried out using a rectangular injection profile. In order to assess the effect of a diffuse front of the injected step on the formation of the shock layers and on their profiles, the same calculations were performed using the injection profile shown in Fig. 7. Fig. 8a shows the front of the elution profiles inside the column at increasing times and, for the sake of comparison,

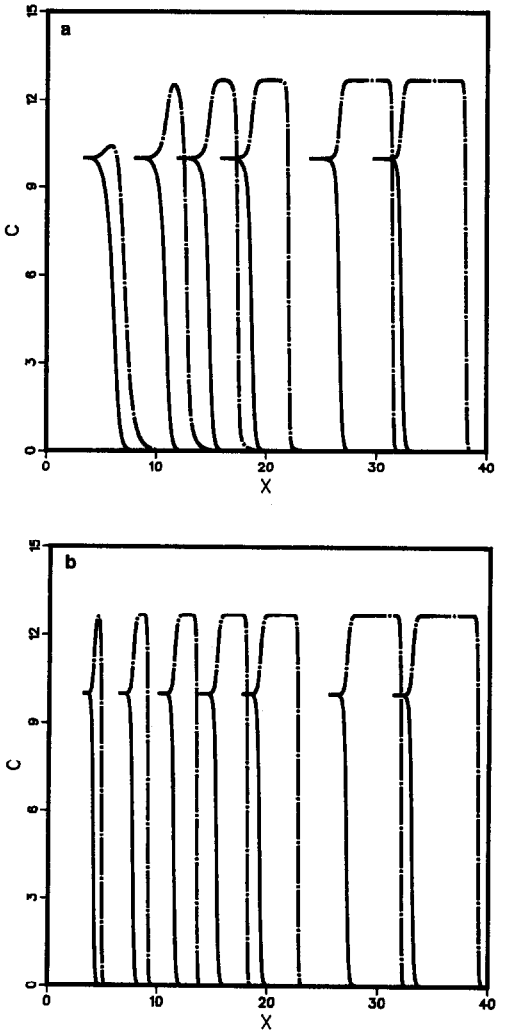

Fig. 8. Concentration profiles inside the column at different times (min). (a) From left to right, 1 = 2.042, 2 = 3.021, 3 = 3.833, 4 = 4.637, 5 = 6.282, 6 = 7.443. (b) From left to right, 1 = 0.842, 2 = 1.578, 3 = 2.352, 4 = 3.149, 5 = 3.956, 6 = 5.583, 7 = 6.801. Calculation parameters as in Fig. 4. The injection concentration is 10 mg/ml for both solutes. X in cm, C in mg/ml.

Fig. 8b shows the front of the elution profiles obtained for a truly rectangular plug injection. In the latter instance, the enriched plateau is more rapidly reached, after only *ca.* 8 cm, whereas in the former the enriched plateau forms more slowly, after *ca.* 16 cm. However, the shock layer profiles and their thicknesses reach the same limit value in both instances, as shown in Fig. 4, which compares the

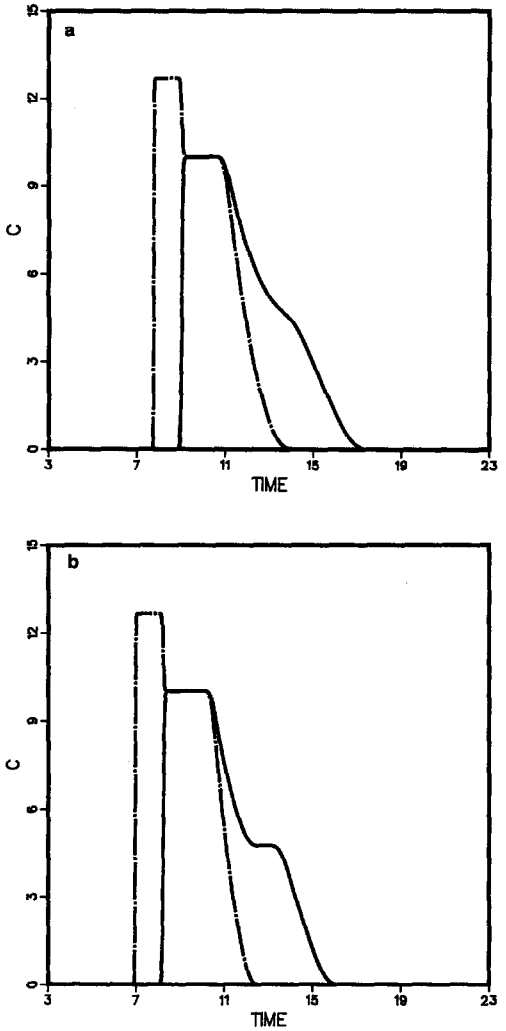

Fig. 9. Complete elution profile of a wide band at the outlet of a 40-cm long column. Solid line, more retained solute; dot-dashed line, less retained solute. Calculation parameters as in Fig. 4. The injection concentration is 10 mg/ml for both solutes. (a) Injection profile as in Fig. 7; (b) the injection profile is a rectangular plug. Units as in Fig. 2.

variation of the shock layer thickness with increasing column length for the two injection profiles. In Fig. 9a and 9b we compare the elution profiles corresponding to the two injection profiles, at the end of a 40-cm long column. Because of the strong selfsharpening effect due to the non-linear behavior of the isotherm, the breakthrough front of a binary mixture band at the outlet of a long enough column is the same in the case of a rectangular plug injection

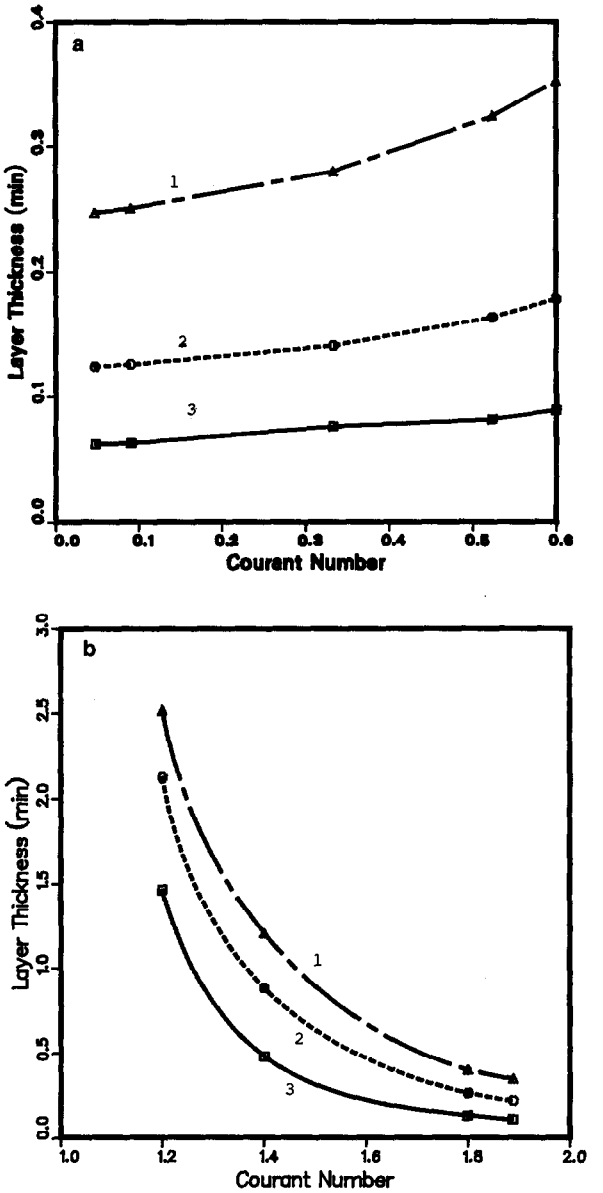

Fig. 10. Plot of the shock layer thickness *versus* the Courant number, $u_z\delta t/\delta x$, where δt and δx are integration increments. Line 1, $H = 0.05$ cm; line 2, $H = 0.025$ cm; line 3, $H = 0.0125$ cm. The other calculation parameters are as in Fig. 4. The injection concentration is 10 mg/ml for both solutes. (a) Calculations made using the Craig (space-like propagation) algorithm described in this work (eqn. 22); (b) calculations made using an alternate algorithm (time-like propagation, ref. 30).

or when the input step has a diffuse instead of a vertical front. The only difference between the elution profiles is in the diffuse, rear parts [16].

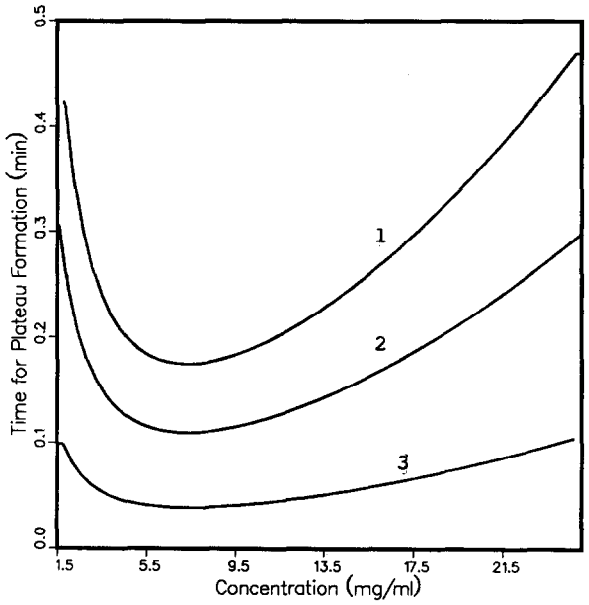

Fig. 11. Plot of the time (min) needed for the formation of the intermediate plateau. Results predicted by eqn. 21. The calculation was done using the same parameters as for Fig. 4. Curve 1, $\theta = 0.002$; curve 2, $\theta = 0.02$; curve 3, $\theta = 0.2$.

Next, we studied the dependence of the shock layer thickness on the parameters used in the numerical calculation. We show in Fig. 10a the variation of the shock layer with the Courant number, $u_z\delta t/\delta x$, where δt and δx are the integration increments, $u_z = u_0/(1 + k'_0)$, u_0 is the mobile phase velocity and k'_0 is the retention factor under linear conditions [30]. Although the shock layer thickness is not constant, which is due to numerical approximations, the dependence is weak and can be neglected as a first approximation. The results presented here have been obtained with a ratio $\delta t/\delta x = 0.2$. For the sake of comparison, we show in Fig. 10b the same result for another calculation scheme [31], which has the great advantage over that used here of requiring approximately ten times less CPU time because the competitive Langmuir isotherm does not have to be inverted [27]. Unfortunately, that scheme exhibits a considerable dependence of the shock layer thickness on $u_z\delta t/\delta x$, and we had to use values of this ratio of the order of 2. Then, very similar results are obtained with both methods. Further calculations have shown that the thickness of the shock layer calculated by the method of orthogonal collocation on finite elements is equal to the one predicted by eqn. 10 and does not depend on the values of δt and δx in the range of values where convergence is achieved [32].

Finally, we compare in Fig. 11 the plots of the time needed for the formation of the enriched plateau *versus* the intensity of the concentration jump in the input step, as derived from eqn. 21. Different values of θ were used. In the numerical calculations, we assume that the enriched plateau is formed when the theoretical value of its concentration is reached at two successive nodes of the grid (for two successive values, k and $k + 1$, of j, see eqn. 22), *i.e.*, if the plateau in a concentration profile along the column is more than $2H$ wide. We note in Fig. 11 that the formation time of the plateau is shorter when large values of θ are used, although the shape of the plot remains unchanged.

The existence of an optimum step height for which the plateau formation time is a minimum is one of the most important features of eqn. 21. Other calculation results (not shown) indicate that, when the HETP is low and a diffuse injection front is used, the minimum is shifted towards higher concentration jumps. When frontal analysis is used for isotherm determination, the height of the successive step should be kept neither too low nor too high to ensure the formation of the enriched plateau at the column outlet and achieve accurate results [18].

Experimental results

Fig. 12a and b compare the dependence of the shock layer thickness on the concentration jump, as calculated from eqn. 10, using the same isotherm parameters as used in Fig. 5 (solid line), and as measured experimentally (symbols). The experimental data in Fig. 12a derived from the detector response (Fig. 13a), by calculating the response differential (Fig. 13b) and determining the width of the peak obtained at half-height. We see that the derivative peaks in Fig. 13b are unsymmetrical. A detailed study of the cause of the asymmetry of the derivative peaks has been made by Rhee and Amundson [15]. In this study we were interested only in the width of the shock layer, not its shape.

The experimental results obtained are in general agreement with the prediction of the shock layer theory and confirm its validity. The shock layer thickness was calculated from eqn. 10, using a value

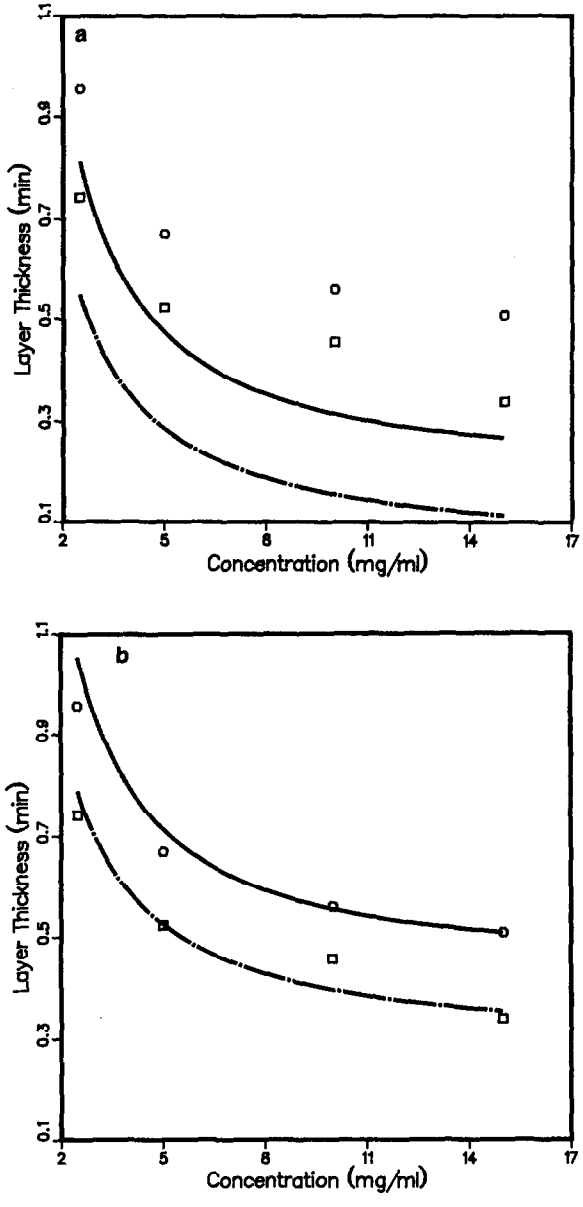

Fig. 12. Comparison between the variations of the shock layer thickness with the concentration jump as predicted by eqn. 10 (lines) and as measured experimentally (symbols). (a) Results. Solid line, more retained compound; dot-dashed line, less retained compound. (b) Same as (a), but theoretical curve shifted upward by 0.25 min.

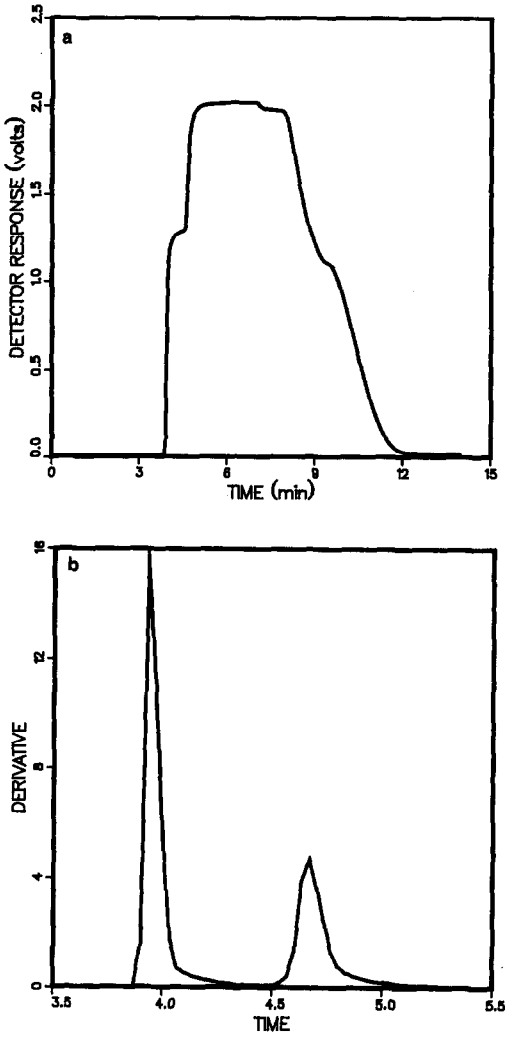

Fig. 13. (a) Elution profile of a wide injection band of a binary mixture and (b) its differential. Time in min.

of $\theta = 0.02$ and a column HETP of 0.01 cm. The experimental and calculated results follow the same trend. However, for a given step concentration, there is a nearly constant difference of 0.25 mm between the measured and predicted thickness. A vertical shift of the theoretical curve by 0.25 mm would bring it into coincidence with the data points. The predicted shock layer is 10–50 s, so a significant detector contribution is improbable, but there might be several reasons for observing a shock layer thickness greater than predicted. For example, the theoretical curve would fit exactly the experimental data points with $H = 0.0275$ cm. The column HETP measured at infinite dilution is different for the two components. An average value is used when apply-

ing eqn. 10 to calculate the second-component shock layer thickness, which is incorrect [15]. More important, the actual system used does not follow the competitive Langmuir behavior, but deviates significantly from it [16,33], which may have an effect on the shock layer thickness. Further investigations are needed to clarify this question.

CONCLUSIONS

Experimental results and those of calculations based on the semi-ideal model confirm the validity of the shock layer theory derived by Rhee and Amundson [12–15]. Shock layers do travel at nearly the same velocity as predicted by the ideal model for the concentration shock itself. The thickness of the shock layer, once it has fully developed, *i.e.*, when a dynamic steady state has been established, depends only on the isotherm, on the height of the concentration jump injected and on the HETP of the column, as shown by eqn. 10. On the other hand, it is independent of the column length.

The development of a shock layer, at the difference of a concentration shock in the ideal model, is not instantaneous. The formation of the enriched plateau of the lesser retained compound is not instantaneous. The time it takes to appear depends on the height of the concentration jump and on the column HETP.

As we have shown, the shock layer theory permits the calculation of the minimum column efficiency necessary to perform an accurate determination of competitive isotherms by frontal analysis. Preliminary experimental results demonstrate the usefulness of the approach. The agreement between the theoretical prediction (eqn. 10) and the experimental data is still not exactly quantitative, however, because of some experimental problems (definition of the HETP in high-concentration chromatography, deviation of the competitive isotherm from Langmuir behavior), problems which have been identified but not yet solved. Further investigations of these problems are in progress. The application of this theoretical study to the determination of the relationship between recovery yield and column efficiency and to the optimization of the experimental conditions in displacement chromatography has also been examined [18].

ACKNOWLEDGEMENTS

We acknowledge Sadroddin Golshan-Shirazi (University of Tennessee) for fruitful discussions. This work was supported in part by grant CHE-89-01382 from the National Science Foundation and by the cooperative agreement between the University of Tennessee and the Oak Ridge National Laboratory. We acknowledge support of our computational effort by the University of Tennessee Computing Center.

APPENDIX I

The total differentials of the two stationary phase concentrations are

$$\frac{Dq_1}{Dc_1} = \frac{\partial q_1}{\partial c_1} + \frac{\partial q_1}{\partial c_2} \cdot \frac{Dc_1}{Dc_2} = \frac{\partial q_1}{\partial c_1} + \frac{\partial q_1}{\partial c_2} \cdot \frac{1}{\xi} \tag{I-1a}$$

$$\frac{Dq_2}{Dc_2} = \frac{\partial q_2}{\partial c_1} \cdot \frac{Dc_1}{Dc_2} + \frac{\partial q_2}{\partial c_2} = \frac{\partial q_2}{\partial c_1}\xi + \frac{\partial q_2}{\partial c_2} \tag{I-1b}$$

and the mass balance equations of the ideal model (eqns. 1 with $D_a = 0$) become

$$\left(1 + F \cdot \frac{Dq_1}{Dc_1}\right)\frac{\partial C_1}{\partial t} + u_0 \cdot \frac{\partial C_1}{\partial x} = 0 \tag{I-2a}$$

$$\left(1 + F \cdot \frac{Dq_2}{Dc_2}\right)\frac{\partial C_2}{\partial t} + u_0 \cdot \frac{\partial C_2}{\partial x} = 0 \tag{I-2b}$$

The directional derivatives for the two components are

$$U_{s,1} = \frac{\dfrac{\partial c_1}{\partial t}}{\dfrac{\partial c_1}{\partial x}} = \frac{u_0}{1 + F \cdot \dfrac{Dq_1}{Dc_1}} \tag{I-3a}$$

$$U_{s,2} = \frac{\dfrac{\partial c_2}{\partial t}}{\dfrac{\partial c_2}{\partial x}} = \frac{u_0}{1 + F \cdot \dfrac{Dq_2}{Dc_2}} \tag{I-3a}$$

These directional derivatives are the characteristic directions, and they give the velocities associated with the corresponding concentrations. The characteristic lines give the propagation trajectories of the different concentrations in the x,t space. Because of the coherence condition [4,16], the directional

derivatives are equal. Then:

$$\frac{Dq_1}{Dc_1} = \frac{Dq_2}{Dc_2} \tag{I-4a}$$

$$\frac{\partial q_1}{\partial c_1} + \frac{\partial q_1}{\partial c_2}\cdot\frac{1}{\xi} = \frac{\partial q_2}{\partial c_1}\cdot\xi + \frac{\partial q_2}{\partial c_2} \tag{I-4b}$$

Rearrangement of eqn. 4b gives eqn. 12a. This equation can be used to find the composition of the mixed zones during the progressive separation of two bands and the profiles of the shock layers.

APPENDIX II

The amount n_1 of the less retained component which elutes pure between the two shocks is given by

$$n_1 = S_1 + S_2 \tag{II-1}$$

where S_1 and S_2 are the integrals of the concentrations C_1 and C_2 along the two shock layers,

$$S_i = \int_{\eta 1}^{\eta r} C_1 \mathrm{d}\eta \tag{II-2}$$

Eliminating n_1 between eqns. 19 and II-1 gives

$$\Delta t = \frac{S_1 + S_2}{c_{1,0}U_1 - c_{2,0}U_2} \tag{II-3}$$

The calculation of S_i is done from the differential of the shock layer thickness [18],

$$\mathrm{d}\eta = \frac{H(1+K)^2}{2u_0K}\left(\frac{C_0+1}{C_0}\cdot\frac{1}{C-C_0} - \frac{1}{CC_0}\right)\mathrm{d}C \tag{II-4}$$

with $K = k'_0/(1 + C_0)$ (eqn. 8a). Thus:

$$S_i = \frac{H(1+K)^2}{2u_0K}\int_{C1}^{Cr}\left(1 + \frac{1+C_0}{C-C_0}\right)\mathrm{d}C$$

$$= \frac{H(1+K)^2}{2u_0K}\left[(2\theta - 1)C_0 + (1+C_0)\ln\left|\frac{1-\theta}{\theta}\right|\right] \tag{II-5}$$

The first-component isotherm is used to calculate S_1 and the decoupled isotherm (eqn. 14) to calculate S_2. Putting these results into eqn. II-3 gives the width of the plateau, Δt.

REFERENCES

1 H.-K. Rhee and N. R. Amundson, *Philos. Trans. R. Soc. London, Ser. A*, 267 (1970) 419.
2 E. Glueckauf, *Discuss. Faraday Soc.*, 7 (1949) 12.
3 G. Guiochon and L. Jacob, *Chromatogr. Rev.*, 14 (1971) 77.
4 R. Aris and N. R. Amundson, *Mathematical Methods in Chemical Engineering*, Prentice-Hall, Englewood Cliffs, NJ, 1973.
5 G. B. Whitham, *Linear and Nonlinear Waves*, Wiley, New York, 1974.
6 A. Jeffrey, *Quasilinear Hyperbolic Systems and Waves*, Pitman, London, 1976.
7 B. C. Lin, S. Golshan-Shirazi, Z. Ma and G. Guiochon, *Anal. Chem.*, 60 (1988) 2647.
8 B. C. Lin, Z. Ma, S. Golshan-Shirazi and G. Guiochon, *J. Chromatogr.*, 500 (1990) 185.
9 Z. Ma and G. Guiochon, *Anal. Chem.*, 62 (1990) 2330.
10 J. N. Wilson, *J. Am. Chem. Soc.*, 62 (1940) 1583.
11 D. DeVault, *J. Am. Chem. Soc.*, 65 (1943) 532.
12 H.-K. Rhee, B. F. Bodin and N. R. Amundson, *Chem. Eng. Sci.*, 26 (1971) 1571.
13 H.-K. Rhee and N. R. Amundson, *Chem. Eng. Sci.*, 27 (1972) 199.
14 H.-K. Rhee and N. R. Amundson, *Chem. Eng. Sci.*, 28 (1973) 55.
15 H.-K. Rhee and N. R. Amundson, *Chem. Eng. Sci.*, 29 (1974) 2049.
16 Z. Ma, A. M. Katti and G. Guiochon, *J. Phys. Chem.*, 94 (1990) 6911.
17 J. M. Jacobson, J. H. Frenz and Cs. Horvath, *Ind. Eng. Chem. Res.*, 26 (1987) 43.
18 Z. Ma and G. Guiochon, *J. Chromatogr.*, 603 (1992) 13.
19 S. Jacobson, S. Golshan-Shirazi and G. Guiochon, *AIChE J.*, 37 (1991) 836.
20 M. D. Levan and T. Vermeulen, *J. Phys. Chem.*, 85 (1981) 3247.
21 C. Thomas, *J. Am. Chem. Soc.*, 66 (1944) 1664.
22 T. Vermeulen, in R. H. Perry, C. H. Chilton and S. D. Kirkpatrick (Editors), *Chemical Engineers' Handbook*, Academic Press, New York, 4th ed., 1963.
23 D. O. Cooney and E. N. Lightfoot, *Trans. Ind. Eng. Chem. Fundam.*, 4 (1965) 233.
24 W. J. Thomas and J. L. Lombardi, *Inst. Chem. Eng.*, 49 (1971) 240.
25 S. Golshan-Shirazi and G. Guiochon, *J. Chromatogr.*, 603 (1992) 1.
26 M. Czok and G. Guiochon, *Anal. Chem.*, 62 (1990) 189.
27 M. Czok and G. Guiochon, *Comput. Chem. Eng.*, 14 (1990) 1435.
28 S. Golshan-Shirazi and G. Guiochon, in F. Dondi and G. Guiochon (Editors), *NATO ASI on Theoretical Advances in Chromatography and Related Separation Methods, Ferrara, Italy, August 1991*, Kluwer, Delft, in press.
29 A. M. Katti and G. Guiochon, *Am. Lab. (Fairfield, Conn.)*, 21, No. 10 (1989) 17.
30 G. Guiochon, S. Golshan-Shirazi and A. Jaulmes, *Anal. Chem.*, 60 (1988) 1856.
31 Z. Ma and G. Guiochon, *Comput. Chem. Eng.*, 15 (1991) 415.
32 Z. Ma and G. Guiochon, in preparation.
33 A. M. Katti, M. Czok and G. Guiochon, *J. Chromatogr.*, 556 (1991) 205.